

# A Parameter for the Selection of an Optimum Balance Calibration Model by Monte Carlo Simulation.

P M Bidgood<sup>1</sup>

CSIR, Brummeria, Pretoria, 0001, South Africa

Prof. A.L.Nel<sup>2</sup>

University of Johannesburg, Auckland Park, 2006, South Africa

**Abstract**—The current trend in balance calibration-matrix generation is to use non-linear regression and statistical methods. Methods typically include Modified-Design-of-Experiment (MDOE), Response-Surface-Models (RSMs) and Analysis of Variance (ANOVA). These methods are used to reduce the number of calibration loads, to identify relevant calibration matrix coefficients, and to avoid or eliminate invalid or detrimental coefficients. The methods are currently focused on the balance loading scheme and the curve-fitting processes. They do not take into account the load dependent uncertainty inherent in the calibration loads, nor do they estimate the uncertainty of the balance when installed in a wind tunnel.

This paper proposes a simulation approach which extends the matrix generation process to take into account both the uncertainties of the applied calibration loads as well as the uncertainty of the electrical response of the balance to these loads. Further, calibration uncertainties are propagated by simulation from calibration through to balance installation to produce uncertainties which may be expected in a wind tunnel. A Performance Weighted Efficiency (PWE) parameter is defined and used to select the best calibration matrix with respect to optimum in-tunnel balance performance. It is proposed that the PWE parameter, either in this form, or with modification, may be an effective balance comparison parameter.

**Keywords**— wind tunnel; balance; calibration; uncertainty;

## I. INTRODUCTION

Current internal balance calibration methods remain varied. These methods range from the determination of calibration coefficients using an OFAT (One Factor at a time) approach combined with a large calibration load set, to various levels of statistical analysis and MDOE approaches [1]. Work has been done on the application of neural network theory as well as corrections for the non-elastic behavior of the balance structure [2].

MDOE methods are directed at obtaining an optimum balance loading scheme that can be applied to effectively determine the coefficients of a pre-defined calibration model: this model may be linear, quadratic or cubic. The most general

of these models is the model recommended by the AIAA and reproduced below in (1) [2].

$$R_i = a_i + \sum_{j=1}^n b_{1,i,j} F_j + \sum_{j=1}^n b_{2,i,j} |F_j| + \sum_{j=1}^n c_{1,i,j} F_j^2 + \sum_{j=1}^n c_{2,i,j} F_j |F_j| + \sum_{j=1}^n \sum_{k=j+1}^n c_{3,i,j,k} F_j F_k + \sum_{j=1}^n \sum_{k=j+1}^n c_{4,i,j,k} |F_j F_k| + \sum_{j=1}^n \sum_{k=j+1}^n c_{5,i,j,k} F_j |F_k| + \sum_{j=1}^n \sum_{k=j+1}^n c_{6,i,j,k} |F_j| F_k + \sum_{j=1}^n d_{1,i,j} F_j^3 + \sum_{j=1}^n d_{2,i,j} |F_j^3| \quad (1)$$

$R_i$  is the electrical response of the  $i$ 'th component,  $F_n$  is the  $n$ 'th load component and the  $a, b, c$  and  $d$ 's are coefficients which need to be determined in the balance calibration process.

The linear, quadratic and cubic terms are easily identified in (1). The additional modulated terms are included to give a degree of functionality to balances whose characteristics are dependent on the sign of the applied load(s). In this paper, only the linear and quadratic terms are considered. Equation (1) then reduces to:

$$R_i = a_i + \sum_{j=1}^n b_{i,j} F_j + \sum_{j=1}^n \sum_{k=j}^n c_{i,j,k} F_j F_k \quad (2)$$

This reduces the number of coefficients that need to be determined for each of the six balance components, ( $F_i$ ), from 96 to 28. Note that (1) is a generalized formulation. Only a subset of this may be valid for any particular balance. The calibration process must therefore not only determine the coefficient values but also the best sub-set of valid coefficients. Determination of the coefficient values is usually done by collecting a range of responses to applied loads for the balance in a calibration rig. A nonlinear least squares fit of this data, using a Gauss-Newton regression scheme for example, is used to determine the values of the coefficients.

RSM and MDOE are useful techniques for comparing calibration loading schemes prior to actual calibration. Numerous statistical approaches enable, inter alia, the

identification of invalid calibration coefficients (e.g. co-linear coefficients) [3], the identification of coefficients with high Variance Inflation Factors [4] and ANOVA to further determine the best set of coefficients for the given data [5][[3]. Although these statistical techniques remain necessary tools, they are not considered by the author to be comprehensive. Some aspects requiring further investigation are described below:

Current statistical techniques are geared towards obtaining a set of valid coefficients which will produce the best “*curve-fit*” for a set of supplied data. Little attention is given to ultimate balance performance in a wind tunnel system. The aim of MDOE is to determine a small but adequate set of calibration loads for a particular calibration model, however, statistical analysis will always demand as much data as possible. This results in conflicting requirements.

Although the statistical techniques are sound, there still remains an element of subjectivity which, if reduced rigorously to an objectively sound result, requires a substantial amount of expertise and costly analysis work. The uncertainty of the applied loads may be included in the current statistical analysis techniques, but it must be included as an average representative value. The load dependent nature of the calibration load uncertainties has yet to be included in current statistical approaches. The load dependency of the uncertainty leads to a fundamental question regarding the relevance of estimated pure error and generalized variance used in statistical analysis and load plan design respectively. The uncertainty of the balance electrical response to the applied loads similarly needs to be included in the analysis.

Current techniques do not implicitly require reference to any standards. Methods for estimating error accumulation, originating in secondary standards, and propagating through the calibration process to the wind tunnel, do not exist in practice.

An inherent assumption is that a valid calibration matrix having back calculated errors (BCE’s) with the lowest standard deviation is the best possible matrix. This drives the inclusion of higher order terms in the search of improving the BCE standard deviation. It should be kept in mind that, in a statistical analysis, a lack-of-fit test is performed relative to the pure error, which is in turn estimated using replicates. It is known that the pure error is load dependent. Therefore, using low load-level replicates may result in a low estimate of the pure error and result in a higher order model with low BCE’s. Using high load-level replicates will overestimate the pure error and result in a lower order model with high BCE’s and an apparently worse balance. The question arises as to the validity of using *any* single-value as an estimate of pure error.

The uncertainty contribution that higher order terms generate in the wind tunnel is not considered in current approaches.

The absence of a comprehensive approach to the calibration of an internal balance is best illustrated by the absence of a universally accepted metric for the comparison of balances. Ewald [6] suggested an equation for the specification of balance accuracy and repeatability.

$$R_i = a_i + \sum_{j=1}^n b_{i,j} F_j + \sum_{j=1}^n \sum_{k=j}^n c_{i,j,k} F_j F_k \quad (2)$$

Where:

$\delta_i$	= Allowed error in component “i” ( $2\sigma$ )
$F_{i,max}$	= Nominal balance range in component “i”
$F_{i,act}$	= Actual load in component “i”
A	= Global accuracy coefficient related to nominal range
B	= Global accuracy coefficient related to actual load
$c_i$	= accuracy coefficient of component “i”
$d_i$	= accuracy coefficient of component “i”
$F_n$	= Actual load of component “n”
$F_{n,max}$	= Nominal load range of component “n”

Conditions for the use and values used in this formula are extensively prescribed. This formulation has been tested and modified and inter-tunnel comparisons have been performed in Europe. Hufnagel [7] looks at the application of this formulation and concludes that although this method of expressing the expanded uncertainty for a wind tunnel balance is possible, the determination of a commonly accepted set of coefficients to be used in the formulation remains problematic. He also suggests the use of an uncertainty matrix to generate uncertainties for each specific load case since the uncertainties are load-dependent. He states that there is no known way of achieving this. One aspect is clear: the use of the word “accuracy” as used in all of these formulations does not provide for the general definition of accuracy as given in AIAA Standard S-071-1995 [8], namely, that “*The word accuracy is generally used to indicate the closeness of the agreement between an experimentally determined value of a quantity and its true value*”.

Other approaches to the generation of an accuracy specification for a balance have been suggested [9]. These are similar in nature to that described by (3).

Calibration rig load uncertainties have been determined by the author according to the AIAA Standard S-071-1995 [8] [10]. The propagation of bias limits into a computed result such as:

$$r = r(X_1, X_2, X_3 \dots \dots, X_j)$$

is given by :

$$B_r^2 = \left( \sum_{i=1}^j \theta_i^2 \cdot B_i^2 \right) + 2\theta_m \theta_n B'_m B'_n \quad (4)$$

$$\text{where } \theta_i = \frac{\partial r}{\partial X_i}$$

and the quantities  $B'_m$  and  $B'_n$  are the portions of the bias limits for measurements of variables  $X_m$  and  $X_n$  that arise from the same sources and are presumed to be perfectly correlated [11], and the bias limits  $B_i$  are estimates at 95-percent confidence of the magnitude of the bias errors in the measurements of the separate variables  $X_i$  [8].

The propagation of precision limits ( $P_r$ ), is slightly simpler but still retains a dependence on the determination of the partial derivatives,  $\theta_i$ . The final uncertainty is then a combination of the bias and precision according to:

$$U_r^2 = (B_r^2 + P_r^2) \quad (5)$$

The use of this approach has been found to be analytically difficult to apply. That is, an accepted approach to the propagation of the load application uncertainties into a calibration matrix and its subsequent effect when used in a wind tunnel environment has yet to be agreed upon. At best, any approach will be analytically or computationally cumbersome.

This overview of current approaches to matrix generation, balance uncertainty, and accuracy estimation, suggests that a single coherent system which caters for all of these requirements in an end-to-end manner has yet to be developed and demonstrated.

It was this somewhat fragmented approach that led the author to investigate the use of a simulation which follows the data path from fundamental calibration rig uncertainties through to the final use of a balance in a wind tunnel. To this end it is assumed that the elemental uncertainties of the calibration system are known. These values are a combination of bias and precision as determined using (5).

## II. THE APPROACH AND SOME ILLUSTRATIVE RESULTS

Fig. 1 illustrates a balance cycle from calibration through to utilization in a wind tunnel. Two distinct systems are illustrated; the calibration system and the wind-tunnel system. The problem is one of propagating elemental uncertainties which originate in the calibration system, through the complete calibration process, to determine uncertainties which will be applicable to a balance installed in the wind tunnel system. In order to do this, uncertainties accumulated in the balance calibration process must be reflected in the calibration matrix, which is moved, along with the balance, from the one system to the other.

It is possible to simulate the balance calibration process in such a way as to include the accumulated effect of all of the elemental calibration uncertainties within the calibration coefficients. It is then possible to transfer these uncertainties into the wind tunnel system, and then add to them additional uncertainty due to the difference in systems, such as, for example, uncertainties in the wind tunnel data acquisition system.

When installed in the wind tunnel, the wind tunnel system will compute, (using a matrix of calibration coefficients,  $M_i$ ), and report a load for a given set of balance voltages generated by the balance under a “perfect” or actual aerodynamic load. Uncertainties due to model inaccuracies, model misalignment, the wind tunnel control system and so forth are not included. The focus at this point is the uncertainty of the reported balance loads.

The uncertainty of the value of a load reported by an installed balance can be estimated by generating numerous loads through a range of matrices,  $(M_i)$ , whose coefficients collectively represent the calibration matrix,  $(M_i)$ , and its uncertainty. In simulated in-tunnel application, the balance response voltages can be varied randomly within their expected uncertainties and be randomly used in combination with these

matrices,  $(M_i)$ , to obtain total load uncertainties which are a result of both the calibration and the wind tunnel systems.

If many random balance loads and their uncertainties are computed using several candidate polynomial functions, the matrix of coefficients for the polynomial function giving the lowest wind tunnel load uncertainties is considered to be preferable. In addition, if the starting point of such a simulation consists of elemental uncertainties, each of which can be traced to a standard, the final uncertainty will be a good estimate of balance accuracy.

In Fig. 1, the points at which MDOE, RSM and ANOVA are applied to matrix generation are indicated. FMI-BCE indicates a balance load reported by the balance as calculated using a calibration matrix which has been generated using these techniques alone.

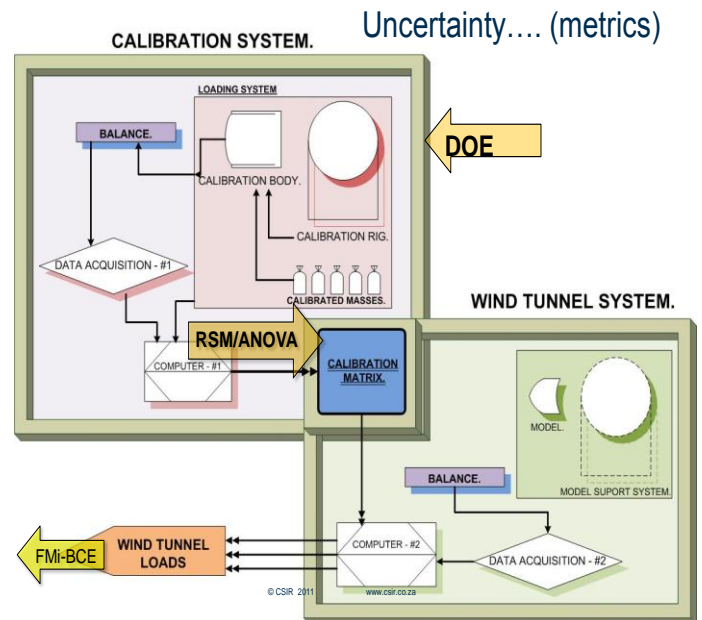


Figure 1. Separate calibration and application environments (systems).

### A. Elemental Uncertainties

The calibration system available for the evaluation of the proposed simulation scheme is a simple gravitational system. The calibration system simplicity makes inclusion of elemental uncertainties in the load calculations relatively easy and computationally fast. A  $\phi 12\text{mm}$  balance calibration body is illustrated in Fig. 2.

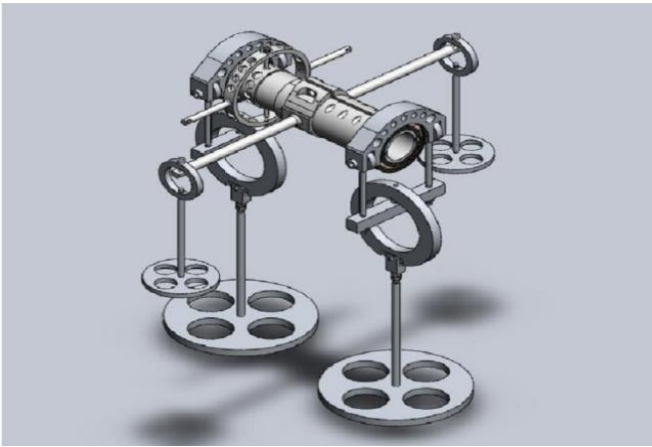


Figure 2. Calibration body for a  $\phi 12\text{mm}$  balance.

In this case the elemental quantities are gravity, the applied masses, the linear and angular dimensions of the calibration body and the leveling instruments. This particular calibration body requires an additional estimate of bearing friction which is not an elemental quantity. With the exception of the bearing friction, all quantities are easily related to a traceable standard.

Each elemental, (dimension, mass etc.), can be expressed as a series of normally distributed random values, whose collective mean and standard deviation matches the mean and standard deviation obtained from a credited metrology facility. These values are used to obtain a range of possible actual loads that could have been applied to the balance for each and every nominal calibration load. Fig. 3 illustrates the expansion of a nominal 211.73 Nm pitching moment load into 1000 possible loads which might have actually been applied. This range of possible load values is a direct result of the accumulation of all of the elemental calibration loading uncertainties. The balance electrical response to this load can be similarly expanded using data on the balance signal uncertainty for each channel. In this case there are six responses.

### B. Static Force Uncertainty

Loads generated in the wind tunnel are actual applied aerodynamic loads. Therefore, from the balance perspective, these aerodynamic loads have no error. (*Uncertainties arising from model misalignment, model inaccuracies or any wind tunnel equipment are not relevant. The focus here is only on the uncertainty of the load reported by the balance.*) A Monte Carlo simulation is used with the expansion of elemental quantities to include the calibration system uncertainties in the calibration matrix in the form of coefficient uncertainties. When installed in a wind tunnel, uncertainties arising from the installed balance signal, (sourced from both the balance itself and the wind tunnel data acquisition system), will propagate through the matrix of calibration coefficients. The propagation of these signal uncertainties can be included in the total uncertainty estimate by, once again, generating a normally distributed expansion for each signal and then passing them through a random selection of coefficient matrices (Min). The resulting computation results in numerous possible loads being computed for each balance output voltage. The uncertainty of

the reported load is captured by the spread of the resulting computed loads.

Fig. 4 shows the suggested simulation path and illustrates the difference between this end-to-end simulation approach and the use of MDOE, RSM and ANOVA alone as illustrated in Fig. 1.

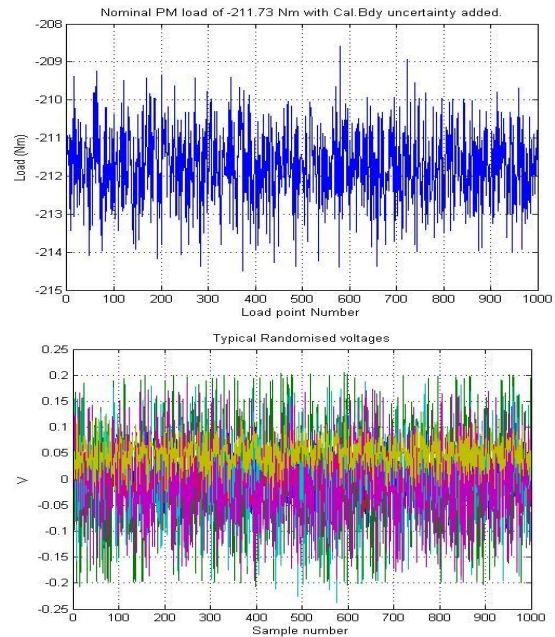


Figure 3. Example of applied load and electrical response expansions.

A characteristic of this approach worth mentioning is that the simulation compliments DOE, RSM and ANOVA methods in such a way that it promises to address some, or all, of the deficiencies discussed in the introduction in a single process. The three outputs labeled FMI-BCE, FMI-FULL and FMI-OPT-PWE, indicate loads calculated through three different calibration matrices. In this paper only the FULL and OPT-PWE matrices are compared in any detail.

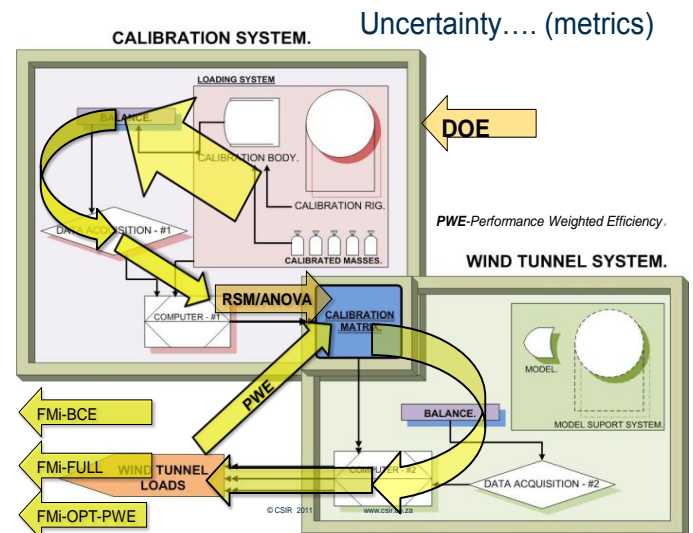


Figure 4. Simulation path for PWE driven matrix generation.

An overview of a simulation scheme that permits the estimation of installed balance uncertainty has been described. It is also a useful tool for the following:

- the evaluation of the effect of load plan design on balance uncertainty
- the improvement in calibration equipment by the identification of fundamental calibration uncertainties which most affect balance uncertainty
- the provision of an alternative tool for the examination of current statistical approaches and methodologies for matrix generation
- the provision of an alternative tool for the examination of uncertainty propagation as described by the AIAA [5].
- the use of installed uncertainty as a balance performance metric
- automated matrix generation

Instead of discussing each of these aspects in detail, the use of the simulation scheme as a tool for automated balance calibration matrix generation is introduced. Note that there is a feedback loop labeled “PWE” in Fig. 4. The PWE parameter is a metric which facilitates the selection of an optimum matrix for some given set of calibration data. This is discussed in the following paragraphs.

### C. Matrix Scanning

One approach to matrix generation [12] includes either a “build-up” of a polynomial coefficient calibration matrix from linear to  $n$ th order using ANOVA to evaluate the relative significance each added coefficient. Another method is to start with a large model, say a third order model (96 coefficients per component), and then to evaluate the relative significance of removing coefficients from the model until a significant set of coefficients has been obtained. Both of these approaches are affected by the fact that the inclusion or exclusion of any coefficient affects the significance of the other coefficients. The order of exclusion or inclusion of coefficients is therefore relevant. In this paper an alternative approach is suggested.

It has been described how a simulation can be used to propagate elemental calibration uncertainties into coefficient uncertainties. This uncertainty data presents an opportunity to develop a polynomial model using a more structured approach than either of those described above. Consider the ratio of the uncertainty to the mean value of a coefficient. Coefficients with small ratios are of more value than those with large ratios. Since the uncertainty and the mean value of a coefficient act on the same balance voltage(s), terms with very high ratios, ( $\gg 1$ ), will contribute more to the computed load uncertainty than to the computed load value. Thus, starting with an infinitely large coefficient uncertainty-to-value ratio (C), coefficients may be discounted depending on the selected value of C. A matrix of coefficients (Mc) is then a matrix which contains only those coefficients whose uncertainty-to-value ratio is below a certain threshold given by the parameter

C. A range of C values can be used to generate a range of candidate polynomials for comparison.

### D. The PWE Parameter

Once a range of calibration matrices, (Mc), have been generated, they need to be comparatively evaluated. In order to do this, the PWE metric is proposed. The following data is available from the simulation:

- The standard deviation of the curve fit Back Calculated Errors (BCEs) for any generated matrix.
- A mean representative uncertainty for each component over a range of random loads.
- Calculation of the confidence interval (CI<sub>rand</sub>) at any random applied load additionally provides a quality of fit metric for off-calibration point loads.

The PWE metric is then formulated as:

$$\begin{aligned} \text{PWE (Performance Weighted Efficiency)} = & \\ & \text{The standard deviation of the BCEs} \\ & + \text{The computed uncertainty for N loads (UNC-tot)} \\ & + \text{The computed Confidence Interval for N loads (CI}_{\text{rand}} \text{)}. \end{aligned} \quad (6)$$

The N loads are chosen to be different from the calibration loads and should be randomly spread throughout the calibration space. Since the uncertainties and confidence intervals are different for each random load, the values used in (6) are defined as:

$$\text{UNC-tot} = \text{Mean} + 2\sigma \quad (7)$$

$$\text{CI}_{\text{rand}} = \text{Mean} + 2\sigma \quad (8)$$

In the results presented in the following paragraph, the computed balance uncertainty already includes a contribution from the random load confidence intervals. The addition of this data again in the PWE function results in a weighting in favor of the confidence interval data.

### E. Test Application

#### 1) The balance and calibration data set.

As an example, matrix generation for a  $\phi 12$ mm balance is considered. This balance was calibrated both at the CSIR and at an independent wind tunnel facility on two fundamentally different calibration systems. The calibrations were in good agreement, both in terms of the calibration BCE standard deviations, and the values of the calibration coefficients.

Calibration BCE data is given for the in-house and independent calibrations in TABLE I. The difference in axial force (AF) values is attributed to hysteresis. In the independent calibration full positive and negative loading was applied to the AF component. In the CSIR calibration, loading was applied in only one direction. This results in lower scatter due to a lower spread of hysteresis. In spite of this difference, the calibration data generated at the CSIR, and used in this example, is considered not to contain information which is

incorrect to the extent that it would directly result in misleading or incorrect results from the simulation analysis.

TABLE I. BCE DATA FOR  $\phi$ 12MM BALANCE.

	BCE data for 12mmK balance (1 $\sigma$ - % calibration Full Scale)	
	INDEPENDENT	CSIR
NF	0.06	0.07
PM	0.10	0.07
SF	0.06	0.06
YM	0.12	0.12
RM	0.99	0.98
AF	0.68	0.58

2) *Fundamental calibration uncertainties.*

Although the calibration masses used at the CSIR are calibrated to a secondary standard, the calibration body itself was not fully measured-up at the time of this writing. Representative uncertainty data were used in the absence of formally determined data. This data is given in TABLE II.

Signal uncertainty attributable to the calibration data acquisition system and balance was assigned a value of  $\pm 2\mu V$ . The same value was used for the wind tunnel data acquisition system.

TABLE II. CALIBRATION SYSTEM UNCERTAINTY DATA.

uncertainty-1 $\sigma$	Item
0.00001	10kg mass uncertainty in kg
0.000002	2kg mass uncertainty in kg
0.0002	Loading station #1 - dimension in meters
0.0002	Loading station #10 - dimension in meters
0.0002	Roll station #11 dimension in meters
0.0002	Roll station #12 dimension in meters
0.0375	Calibration body radius in meters
0.1	Pitch leveling in degrees
0.1	Roll leveling in degrees
0.1	Axial Force cable leveling in degrees
0.1	Axial Force cable yaw angle in degrees
0	Axial force pulley friction

1) *Feasible limits.*

Expanded calibration load uncertainties, such as that shown in Fig. 3, enable the generation of bounding values on what might be expected from a calibration. This can be done prior to any actual calibration and can be a useful tool for calibration system improvement. Consider the maximum deviation from the mean and assume this to be the final resulting curve fit error at this load point, (and similarly for all other calibration loads). It follows that, using these maximum values as an upper bound of what the final curve fit error might be, an upper bound of the calibration BCE's can be calculated. Several other options are also possible. For example, a random selection of single data points may be taken from each calibration load's expanded data, or, the standard deviation of the variance for any given load can be used as an estimate of what the final calibration BCEs might be.

Several horizontal lines are visible in the following simulation results. Each of these represents an estimate of calibration BCEs using a range of possible values as have been described above. These curves are labeled 2smax, 2srand and 3srand. These are not discussed further except to comment that it is at least expected that the final data for the UNC-tot, CalBCE and CIsrand values fall within, or close to, these predictive lines.

A range of C values were used to generate a set of candidate matrices. It should be noted that the last point on the x-axis, in the data plot shown in Fig. 5, is actually an infinite ratio (C=1e99) – not a ratio of 30 as is used on the plots. The plotting limitations are obvious.

A value of C=0.05, for example, is interpreted in the simulation as a request to retain only those coefficients whose uncertainty is less than 5 per cent of their mean value. It should be noted that because the inclusion or exclusion of any coefficients directly affects the values of the other coefficients, the 5 per cent level of coefficient retention needs to be approached incrementally.

2) *Simulation Results.*

The plots shown in Fig. 5, 6 are the same, except that the region above a C value of 5 on the x-axis has been omitted in the second plot. The only plotted data discussed here are the PWE (Performance Weighted Efficiency), CalBCE (Back calculated Curve fit Errors), CIsrand (Confidence Interval of random off-calibration loads) and UNC-tot (uncertainty obtained for a number of random loads).

In Fig. 6 a region with a significantly lower PWE value can be seen. The region of interest is below a C value of 1 on the horizontal axis. This is reasonable since it is intuitively expected that a meaningful coefficient will have a mean value at least greater than its uncertainty. In this case the lowest PWE value occurs if only those terms whose variance is between 5 and 10 per cent of the terms value are retained. Fig. 7 shows this point of minimum PWE value. It can be seen that although allowing the inclusion of more coefficients in the calibration model, (increasing C), will result in a decreasing, and hence improving, BCE value, it also results in increasing the final balance uncertainty (UNC-tot). This also occurs in the off-calibration point confidence intervals (CIsrand). This is a compelling indication that calibration coefficients which give the best curve-fit of the calibration data, (as determined using the curve-fit BCE's as the metric), do not necessarily result in the best *operational* calibration matrix.

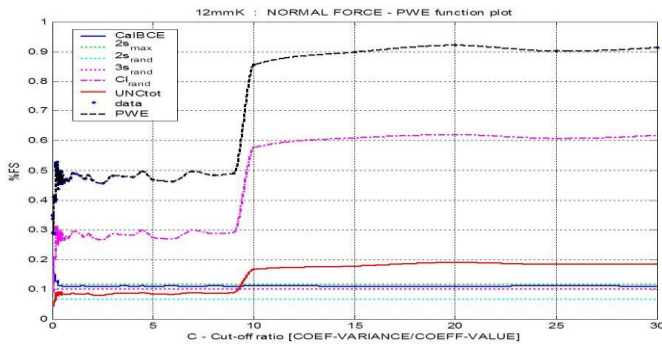


Figure 5. Data for a C scan of a  $\phi 12\text{mm}$  balance ( $C_{\text{max}}=1e99$ ).

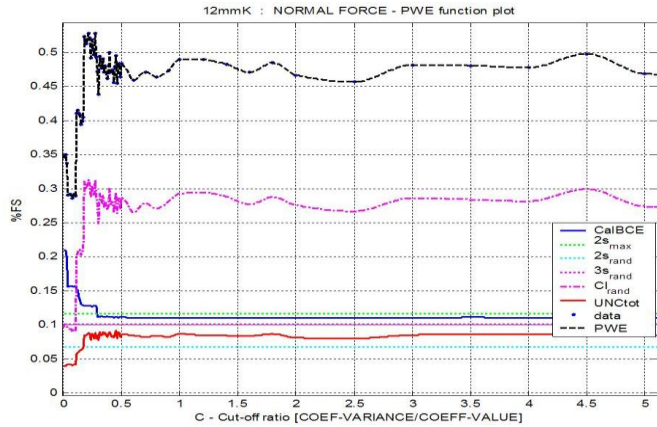


Figure 6. Data for a C scan of a  $\phi 12\text{mm}$  balance ( $C_{\text{max}}=5$ ).

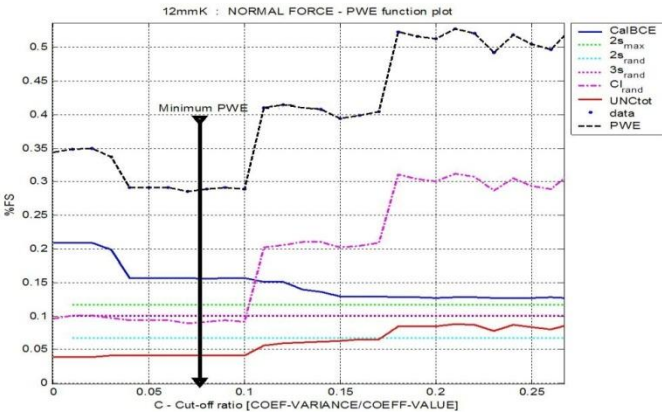


Figure 7. Optimum C for  $\phi 12\text{mm}$  balance (Normal Force).

### 3) Comparison of Some Calibration data.

Some comparative data is supplied in TABLE III. The “FULL” matrix is a 26 term matrix, ( $C=1e99$ ), whilst the “OPT” matrix is one that has been reduced using the C value at the point of minimum PWE.

The higher value of BCE for normal force (NF - full matrix) when compared with the data in TABLE I can be explained by additional on-going work on matrix generation. This work is not pertinent to this paper. The improvement in predicted balance uncertainty when using a PWE optimized matrix can be seen in TABLE III.

TABLE III. COMPARATIVE DATA FOR NORMAL FORCE.

12mmK Balance - (Small Cal. Errors)					
OPT. MATRIX			FULL matrix(26)		
BCE( $1\sigma$ ) [%FS]	UNC( $2\sigma$ ) [%FS]	Coeffs.	BCE( $1\sigma$ ) [%FS]	UNC( $2\sigma$ ) [%FS]	Coeffs.
0.16	0.09	5	0.11	0.61	26

The increase in BCE value for the “OPT.MATRIX” compared to those for the “FULL matrix(26)” is considered small relative to the improvement in operational uncertainty. Note also that the UNC( $2\sigma$ ) uncertainty for the “OPT” matrix is less than the calibration BCE( $1\sigma$ ) value. The reverse is true for the “FULL” matrix. The reason for this is that the calibration BCE data contains all the actual calibration rig loading errors. The UNC value however has no loading error: it contains only contributions from the calibration errors reflected in the matrix terms, the installed balance signal uncertainty, and the confidence interval data obtained from a range of simulated random loads. “Actual” calibration loading error has been eliminated except for its contribution to uncertainty of the coefficients – and this effect has been minimized by model selection.

### 4) Wind tunnel test data.

Comparisons such as that provided in TABLE III are interesting and can be used to further investigate balance calibration matrix generation; however, the final performance or usefulness of this alternative matrix needs to be demonstrated on real wind tunnel test data. In the following, only the axial force component is compared. This is done because the test data that was made available was a roll polar of an almost symmetrical body at low pitch angles. The resulting loads are therefore low. The result is that, apart from the differing uncertainty bands for each of the matrices, the computed loads are practically identical for all the components. Axial force (AF) loads are also low, (approximately 8% of balance full scale), but differences are discernible.

Fig. 8 shows the AF data processed through both the full and PWE-optimized matrices. Uncertainty values are computed at each data point and plotted as bands about the data.

For the full matrix, the uncertainty band is around 0.25N wide and for the PWE matrix the band is around 0.1N wide. A total load variation during the polar of around 0.4N is indicated using the full matrix, whilst it is closer to 0.3N for the PWE matrix. (Data is read from the graph at data points just beyond  $1.4e4$ ). These differences are small, but it must be remembered that they are generated at a maximum load level of less than 8 percent of the balance full scale value of 100N. The total variation in load during the polar is less than 0.7 percent.

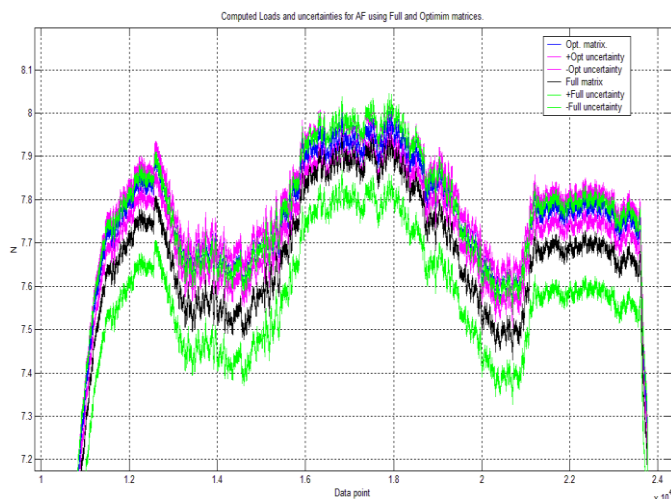


Figure 8. Axial force (AF) loads computed using a full and a PWE-optimized matrix.

The optimized AF uncertainty in this test region can be expressed as approximately  $\pm 0.05\%$  of the balance AF full scale. The standard deviation of the calibration BCEs for AF was reported as 0.71% of full scale. The significantly larger BCE value can be attributed to numerous factors. The most pertinent of these is the fact that the uncertainties calculated here are load dependent. The load dependent uncertainty results in low uncertainties at low loads. Significantly higher values of AF uncertainty can be expected at higher AF loads. The absence of any direct relationship between BCE values and uncertainty values is important.

Finally, it is interesting to see that the optimized matrix data falls either on, or just inside, the upper uncertainty band of the full second order matrix.

##### 5) The PWE parameter as a metric.

By considering the plots in Fig 4, 5 and 6, the effectiveness of the PWE parameter as a general balance metric becomes apparent. The parameter is the sum of the curve-fit back calculated errors (BCE), a value for the estimated installed balance uncertainty (UNC-tot), and a 95% confidence interval value ( $CI_{rand}$ ). The use of BCE alone to measure the effectiveness or quality of a calibration is clearly misleading because in this case it will result in a considerably larger operational uncertainty. An inadequate loading scheme will cause high values of  $CI_{rand}$ . Over- or under- fitting of the data will also result in raised values of  $CI_{rand}$ . In the absence of this, under-fitting will be indicated by the BCE. Thus, provided that the fundamental calibration uncertainties are determined and related to a secondary standard, no manipulation of the final value of the PWE function can be performed. The following characteristics of the PWE metric generated by this approach are noted:

- generation of the PWE metric *requires* a reference to secondary standards

- Manipulation or interpretation is difficult or impossible – it is objective
- It is calibration system independent - it depends only on calibration load and balance signal uncertainties
- It can be automated; this implies that the need for human judgement is eliminated
- It provides a direct form of uncertainty matrix for the generation of on-line uncertainty data for each load point at low computational cost.

It should be noted that this simulation approach is not intended to replace the currently used statistical methods. It is an additional end-to-end process intended to augment and assist in the further development of existing methods. The simulation process as presented here still requires additional procedures to internally identify aliasing or co-linearity for example. Examination and planning of calibration load schemes still relies heavily on RSM and DOE techniques. In fact, the calibration load plan and the calibration system, (and of course the balance itself), now become the only factors which can be used to improve the balance performance metric(s).

### III. DISCUSSION

It often occurs with the proposal of any new approach that more questions are raised than are answered. This simulation approach is no exception.

The first question the author was faced with was that of simulation size and computational time. To answer this, simulations were done with sizes ranging from 50 point expansions to 1000 point expansions. It was seen that after around 200 points there was no appreciable change in the simulation results.

The question as to the effects of inadequately randomized data can only be answered by the statement that up to 1000 random data points with a normal distribution having no repeats is achievable. Larger simulations may require additional attention to this aspect. The data presented in this paper used a 300 point simulation. This means that, at any single point, data is expanded to 300 random points, that 300 matrices are generated for each (Mi) case, that 300 random loads were used in the estimation of balance uncertainty and so forth. A scan using the C value range 0.01, 0.05, 0.1, 0.2, 0.3, 0.5, 0.7, 1, 2, 5, 8, 10, 15, 20 and 1e99 takes around 2 to 3 hours on an Intel i5 processor in a laptop computer. The more detailed plots presented in this paper containing 75 C values are best generated overnight.



Because the data flow is simulated, aspects of the data may be investigated at any stage in the process. For example, identification of the terms removed for different values of C may be compared with computed parameters or with parameters from matrices generated using a statistical approach alone. The coefficients retained for each C were used to produce a table such as that given in Fig 9. Fig. 9 is a

Similarly, a sixteen percent uncertainty-to-value ratio, (or C=0.16), results in the retention of ten coefficients.

Fig. 10 shows the full C value scan with a plot of several parameters computed using the valid coefficients at each C value. Alignment of the graph with the table is approximate. The relevance and effect of each term may be investigated in plots such as these. The calibration coefficients for NF range

		Back	Fore	Step	0.01	0.02	0.03	0.04	0.05	0.06	0.07	0.08	0.09	0.1	0.11	0.12	0.13	0.14	0.15	0.16
NF	A	1	1	1	1	1	1	1	1	1	1	1	1	1	1	1	1	1	1	1
PM	B	0	0	0	0	0	0	0	0	0	0	0	0	0	0	0	0	0	0	0
SF	C	1	1	1	1	1	1	1	1	1	1	1	1	1	1	1	1	1	1	1
YM	D	1	1	1	0	0	0	0	0	0	0	0	0	0	0	0	1	1	1	1
RM	E	1	1	1	0	0	0	1	1	1	1	1	1	1	1	1	1	1	1	1
AF	F	1	1	1	0	0	0	0	0	0	0	0	0	0	0	0	0	0	0	0
NF.NF	AA	0	0	0	0	0	0	1	1	1	1	1	1	1	1	1	1	1	1	1
PM.PM	BB	0	0	0	0	0	0	0	0	0	0	0	0	0	0	0	0	0	0	0
SF.SF	CC	1	1	1	0	0	1	1	1	1	1	1	1	1	1	1	1	1	1	1
YM.YM	DD	0	0	0	0	0	0	0	0	0	0	0	0	0	0	0	0	0	0	0
RM.RM	EE	0	0	0	0	0	0	0	0	0	0	0	0	0	0	0	0	0	0	0
AF.AF	FF	1	1	1	0	0	0	0	0	0	0	0	0	0	0	0	0	0	0	0
NF.PM	AB	0	0	0	0	0	0	0	0	0	0	0	0	0	0	0	0	0	0	0
NF.SF	AC	1	1	1	0	0	0	0	0	0	0	0	0	0	0	0	1	1	1	1
NF.YM	AD	0	0	0	0	0	0	0	0	0	0	0	0	0	0	0	0	0	0	0
NF.RM	AE	0	0	0	0	0	0	0	0	0	0	0	0	0	0	0	0	0	0	0
NF.AF	AF	1	1	1	0	0	0	0	0	0	0	0	0	0	0	1	1	1	1	1
PM.YM	BD	0	0	0	0	0	0	0	0	0	0	0	0	0	0	0	0	0	0	0
PM.RM	BE	0	0	0	0	0	0	0	0	0	0	0	0	0	0	0	0	0	0	0
PM.AF	BF	0	0	0	0	0	0	0	0	0	0	0	0	0	0	0	0	0	0	0
SF.YM	CD	1	1	1	0	0	0	0	0	0	0	0	0	0	0	0	0	0	1	1
SF.RM	CE	1	1	1	0	0	0	0	0	0	0	0	0	0	0	0	1	1	1	1
SF.AF	CF	0	0	0	0	0	0	0	0	0	0	0	0	0	0	0	0	0	0	0
YM.RM	DE	1	1	1	0	0	0	0	0	0	0	0	0	0	0	0	0	0	0	0
YM.AF	DF	0	0	0	0	0	0	0	0	0	0	0	0	0	0	0	0	0	0	0
RM.AF	EF	0	0	0	0	0	0	0	0	0	0	0	0	0	0	0	0	0	0	0
CONST	CONST	1	1	1	0	0	0	0	0	0	0	0	0	0	0	0	0	0	0	0
		Back	Fore	Step																

Figure 9. Sub-section of a coefficient validity map for a balance component. (normal force (NF))

small section of Fig. 10 and is provided for clarity.

The first two columns identify a particular polynomial coefficient. The rows indicate the validity of the coefficients depending on the C value given in the topmost row. The next three columns show automatically selected terms for three different matrix generation schemes using statistics only. The first “Back” column is a backwards elimination scheme. The second is a forwards scheme and the last is a step-wise scheme [12]. In all schemes an Alpha of 0.05 was used. Active coefficients have a unit value and are shaded, whilst invalid or eliminated coefficients are zero and have no shading. For example, a one percent uncertainty-to-value ratio requirement for the coefficients, (or C=0.01), results in the retention of only the NF and SF coefficients.

from the full 26 term matrix, (FULL matrix), on the right hand side of the table, up to, and beyond, the optimum number of coefficients. On the upper end of the scale, (FULL matrix), it can be seen that seven coefficients have very small values relative to their uncertainties and are removed at a C value of between 9 and 10. From the accompanying plot, the effect on the BCE value is seen to be negligible. Numerically, differences are seen only in the fourth decimal place. The effect on balance installed uncertainty, however, is to drop it from 0.65 percent to 0.28 percent. The primary driver of this drop in uncertainty is the improved confidence interval of the curve fit generated at random load points during the simulation.



Towards the centre of the table in Fig. 10, in the C value range of 0.35 to 0.4, a set of coefficients most closely matching those obtained using the forward, backward or stepwise statistical approach is marked. Terms included in the simulation but excluded in the statistical approach are shaded (yellow).

Two further significant drops in installed balance uncertainty can be seen at points around C=0.15 to 0.18 and C=0.1 to 0.13 respectively. The addition of the NF.AF cross-coupling term can be seen to be the main source of the uncertainty jump at the latter location whilst the YM.RM cross-coupling term is the responsible term at the former location. It is interesting to see that both of these terms are included in the statistically generated model.

The location of the minimum PWE value occurs at a C value of around 0.07. This C value identifies an optimal set of coefficients for NF, three of which are linear and two of which are quadratic. The quadratic terms are hierarchical in that their linear terms are also included. Non-linear components such as axial force (AF) and rolling moment (RM) generally contain numerous valid cross-coupling terms.

“Bumps” in the plot of Fig. 10 prompted an additional investigation into the stability of the simulation. To this end, a simulation at a C value of 0.1 was repeated 10 times. It can be seen in Fig. 10 that, at some point close to this C value, the NF\*AF cross-coupling coefficient is considered valid and is included.

The results of repeated simulations at C=0.1 are shown in Fig. 11. The two bumps in the plot indicate that, due to the nature of the simulation, small variations prevent the identification of valid terms at very precise values of C. In this case the C value for a valid NF\*AF cross-coupling coefficient is close enough to 0.1 to cause it to be included in two of the ten simulations. For the remainder of the data, the repeatability from simulation to simulation is sufficient to validate the inferences made thus far.

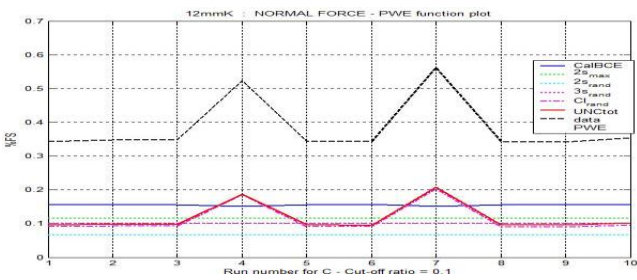
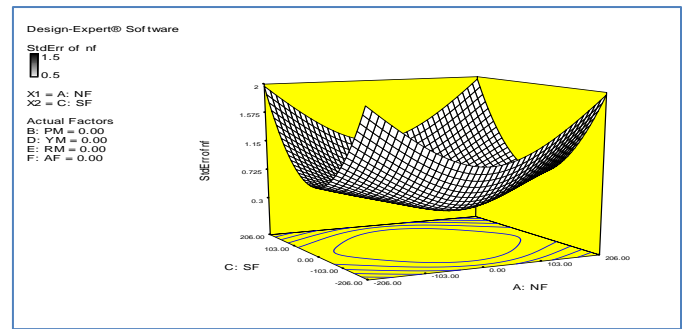


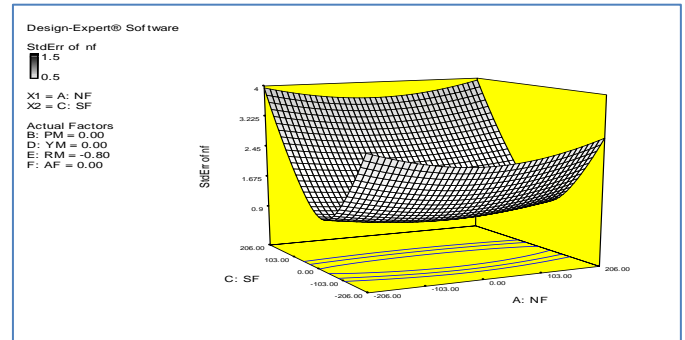
Figure 11. Stability of repeated simulations.

Comparisons between statistically derived matrices and PWE derived matrices can also be investigated by performing a statistical evaluation of the PWE matrix. It should be noted at this point that the balance presented in this example is not of a particularly high standard. To some extent this was desirable because any techniques employed, either for matrix generation, or for accuracy estimation, should be capable of identifying such cases. Standard error plots are provided below in Fig. 12 A and B for nf using a backwards term elimination scheme [12] only. Fig. 13 A and B are the same

plots generated using terms as determined using the minimum PWE parameter approach.

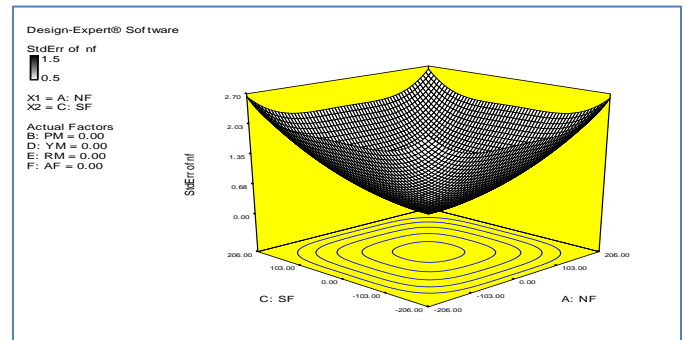


A.)  $PM=YM=RM=AF=0$

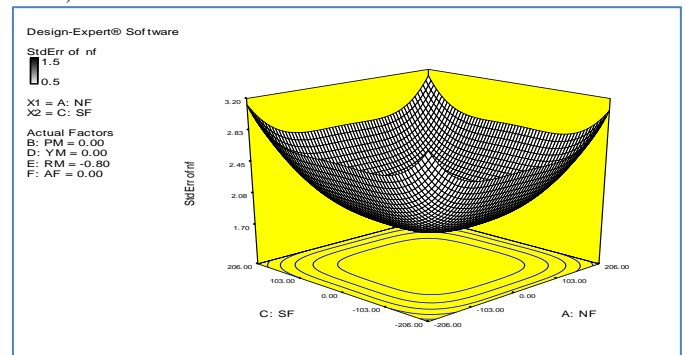


B.)  $PM=YM=AF=0$  and  $RM=-0.8Nm$

Figure 12. Standard Error for nf as a function of SF and NF using Backwards elimination.



A.)  $PM=YM=RM=AF=0$



A.)  $PM=YM=RM=AF=0$

Figure 13. Standard Error for nf as a function of SF and NF by the minimum PWE approach.

The significant difference in the shape of these standard error surface plots, apart from the imposed load dependence in the PWE-optimized matrix, requires a more substantial explanation than is possible in this paper.

#### IV. CONCLUSION

A Monte Carlo simulation approach was used to model the propagation of uncertainty of a balance from calibration through to wind-tunnel installation. The Performance Weighted Efficiency (PWE) parameter is defined as a combination of the calibration BCEs, the installed uncertainty and the average 95% confidence interval for random loads throughout the calibration space as given in (6). The PWE parameter is further used as a metric to determine an optimum set of calibration coefficients based on predicted in-tunnel balance performance.

The number of coefficients selected for optimum in-tunnel performance, as determined using the coefficient uncertainty-to-value ratio (C) at the point of minimum PWE value, is generally fewer than are determined using current statistical methods. The inclusion of load-dependent uncertainty data and the effect on installed balance uncertainty plays a significant role in the selection of matrix coefficients. This is apparent when comparing standard error plots of a matrix generated using current statistical methods and a matrix obtained using the PWE metric.

An additional and useful metric is defined as the ratio of the average confidence interval at many random points within the calibration space to the average confidence interval at calibration points. The difference in this ratio between a fully populated second order matrix and one that has been optimized is significant.

Comparisons have largely been limited to a fully populated second order quadratic and a PWE optimized version of the same matrix. More extensive investigations involving the comparison of statistically derived matrices and PWE derived matrices are required.

The simulation of uncertainty propagation in a balance from calibration to installation additionally provides a useful model for, inter alia, calibration system improvement, automated matrix generation, a basis for balance comparisons, the development of meaningful metrics, balance design investigations and the generation of direct-form uncertainty matrices.

Using this simulation approach, attempts to align the different methodologies that are currently available can serve

to promote a fuller understanding of internal wind tunnel balances and their accuracies. This increased understanding can be used to develop commonly accepted metrics and methodologies. In turn, this can only result in improved wind tunnel data quality.

#### REFERENCES

- [1] Raymond Bergman, Iwan Phillippen. "An experimental comparison of different load tables for balance calibration." Williamsburg, Virginia : 7th International Symposium on Strain-Gauge balances, 11-13 May,2010.
- [2] AIAA. Recommended Practice. "Calibration and Use of Internal Strain-Gage Balances with Application to Wind Tunnel testing." s.l. : American Institute of Aeronautics and Astronautics , 2003. Vol. 1. ISBN 1-56347-646-0.
- [3] N.Ulbrich, T.Volden. "Development of a New Strain-Gage Balance Calibration Analysis Capability at NASA Ames Research Center." Zwolle,The Netherlands : 6th International Symposium on Strain-Gage Balances, 2008.
- [4] O'brien, Robert M. "A Caution Regarding Rules of Thumb for Variance Inflation Factors." s.l. : Springer, 2007. Vols. Quality & Quantity (2007) 41:673-690, DOI 10.1007/s11135-006-9018-6.
- [5] T.Volden, N.Ulbrich. "Regression Model Term Selection for the Analysis of Strain-Gage Balance Calibration Data." Williamsburg, Virginia : 7th International Symposium on Strain-Gauge balances, 11-13 May,2010.
- [6] Ewald, Bernd. "The Uncertainty of Internal Wind Tuinnel Balances. Definition and Verification." Darmstadt,Germany : 3rd International Symposium on Strain-Gauge Balances., 13-16 May,2002.
- [7] Hufnagel, Klaus. "Common definition of Balance Accuracy and Uncertainty." Williamsburg, Virginia : 7th International Symposium on Strain-Gauge Balances, 11-13 May,2010.
- [8] AIAA. Assessment of Wind Tunnel Data Uncertainty. 1995. S-071-1995.
- [9] David M Cahill. "Balance Calibration Uncertainty - Introduction to discussion on standardisation." Presentation. Zwolle, The netherlands : 6th International Symposium on Strain-Gauge balances, 5-8 May,2006.
- [10] P.M.Bidgood, C.M.Johnston. "Uncertainty project." *Report*. Pretoria,SA : CSIR, April,2005. DEF 2005/033.
- [11] Coleman, H.W. and steele, W.G. "Experimentation and Uncertainty Analysis for Engineers." New York, NY : John Wiley & Sons, Inc., 1989.
- [12] STAT-EASEInc. Design-Expert 7. [Statistical Analysis Software] Minneapolis,MN 55413 : s.n.
- [13] T.Volden, N.Ulbrich. "Development of a New Software Tool for Balance Calibration Analysis." Paper presented at 25th AIAA Aerodynamic Measurement Technology and Ground Testing Conference. San Francisco,California : s.n., AIAA 2006-3434, June 2006.
- [14] Mark E. Kammeyer and Mathew L. Rueger. "Estimation of the Uncertainty in Internal Balance Calibration Through Comprehensive Error Propagation." Paper presented at 26th AIAA Aerodynamic Measurement Technology and Ground Testing Conference. Seattle, Washington : s.n., AIAA 2008-4029, June 2008.